

# DYNAMIC SIMULATION OF A ROTORCRAFT HYBRID ENGINE IN SIMCENTER AMESIM

Ioannis Roumeliotis, Theoklis Nikolaidis,  
Vassilios Pachidis

Cranfield University, UK

i.roumeliotis@cranfield.ac.uk

Olivier Broca, Deniz Unlu

Siemens Industry Software, France

olivier.broca@siemens.com

## Abstract

This paper assesses a series hybrid propulsion system utilizing a recuperated gas turbine configuration. An adapted engine model capable to reproduce a turboshaft engine steady state and transient operation is built and used as a baseline for a recuperated engine. The recuperated engine presents a specific fuel consumption improvement of more than 15% at maximum continuous rating at the expense of surge margin which is reduced. An Oil and Gas (OAG) mission of a Twin Engine Medium helicopter has been used for assessing the hybrid configuration. The thermo-electric system brings a certain level of flexibility allowing for the recuperated engine to operate for high take-off weight cases. If envisioned 2025 technology is considered the fuel benefit of the series hybrid recuperated configuration for the OAG mission is in the range of 5%. The integrated system models (gas turbine, electric and heat exchanger systems) are built in Simcenter Amesim, a system modelling platform allowing for both steady state and dynamic simulation.

## 1. INTRODUCTION

There is a growing concern over the environmental impact of aviation explained by the fast growth of the global aviation traffic. An average 4% annual growth is manifested, while the 2035 global traffic is forecasted to be twofold that of 2016<sup>[1]</sup>. Rotorcrafts, that currently fly an average of 1,500,000 flight hours consuming 400,000 tonnes of aviation fuel annually, are going to be part of this growth. Specifically helicopters are seen as a quick and safe way to transport patients between hospitals<sup>[2]</sup>, while the traffic for passenger transport/air taxi, which has been a marginal activity until now, is expected to boom in the near future with a two to three-fold increase in the period of 2015-2020<sup>[3]</sup>. Therefore, the rotorcraft fleet contribution to environmental impact is becoming a concern and measures to reduce it are investigated and assessed.

The development of new technologies can potentially hinder the environmental emissions of the aviation industry. Several ways to tackle this challenge have been proposed ranging from changing the aircraft operational procedures<sup>[4]</sup> to

radically changing the aircraft and propulsion system architecture<sup>[5]</sup>. The “More Electric Aircraft” (MEA) concept is expected to be in the forefront of this change, given that already pneumatic and hydraulic aircraft systems are replaced by electric systems<sup>[6]</sup>. On longer term hybrid electric and universally electric aircraft are considered as promising concepts for addressing the NASA N+3<sup>[7]</sup> goals and the Strategic Research Innovation Agenda<sup>[3]</sup> as discussed by Vratny et al.<sup>[8]</sup>.

Thermo-electric or hybrid powerplants capitalize on the use of efficient core engine alongside electric energy storage systems. Thermo-electric configurations bring a certain level of flexibility into the powerplant design and the vehicle as a whole, since the engine may operate in more favourable operating points throughout the mission (high power settings – low specific fuel consumption – sfc), providing propulsive power and electric power in several systems at the same time. This flexibility is of interest for rotorcrafts since typical helicopter cruises between 55% to 65% of the installed power for around 80% to 90% of the helicopter flight<sup>[9]</sup>, operating at high sfc points. Additionally hybrid electric power systems for rotorcrafts may offer high reliability and lower maintenance cost, mainly due to eliminating or reducing the gearboxes and transmissions, components that do not have graceful failure modes. Another interesting aspect is that in the case of hybrid configuration the supplemental power may be provided by the battery pack rather than the engine itself in case of OEI (One Engine Inoperative) operation, adding to the safety and reducing the need for over-sizing the engine. These advantages come with increased weight

---

### Copyright Statement

*The authors confirm that they, and/or their company or organization, hold copyright on all of the original material included in this paper. The authors also confirm that they have obtained permission, from the copyright holder of any third party material included in this paper, to publish it as part of their paper. The authors confirm that they give permission, or have obtained permission from the copyright holder of this paper, for the publication and distribution of this paper as part of the ERF proceedings or as individual offprints from the proceedings and for inclusion in a freely accessible web-based repository.*

and complexity of the whole propulsion system, thus for assessing the performance of a hybrid propulsion system the increased weight of the helicopter should be considered.

Another way to address the increased specific fuel consumption during part-load operation of helicopters is the regenerative / recuperated cycle. The deployment of regenerative technology for enhancing the operational capabilities of helicopters, specifically for military use, has been of interest since 1960s<sup>[10]</sup>. Fakhre et al.<sup>[11]</sup> demonstrated that the conceptual recuperated helicopter has the potential to significantly improve the maximum attainable range capability, achieving a significant reduction in mission fuel burn. The advantages of the recuperated cycle come with increased weight, complexity and lower specific power due to the heat exchanger pressure losses. The latter is important if an existing engine is considered for modification, since its power ratings are expected to significantly decrease, thus it may not be capable to power existing helicopters. Additionally the dynamic behaviour of the engine is expected to change due to the thermal inertia of the heat exchanger. A thermo-electric powerplant utilizing a recuperated cycle is expected to negate the effect of heat exchanger pressure losses to the engine power output, thus making this concept more interesting since existing engines can be modified decreasing the development time and cost.

For assessing this type of configuration an integrated series hybrid – electric recuperated turboshaft configuration for rotorcraft application is modelled and simulated. The recuperated engine model built is based on publicly available experimental data of a T700-GE-700 engine test rig<sup>[12]</sup>. A model of this engine adapted to steady state experimental data and capable to reproduce with very good accuracy the steady state and transient operation of the engine throughout the whole operating envelope is built. Following a recuperated version of the engine is developed and its performance and dynamic behaviour are calculated and discussed. Following a series hybrid configuration utilizing the recuperated engine is built. The hybrid configuration is assessed in terms of performance and engine operability for a typical Twin Engine Medium (TEM) helicopter mission. The effect of weight increase due to hybridization and recuperation on the fuel burn benefit is quantified and the degree of hybridization for different operating conditions is calculated.

The simulation of the different systems (gas turbine, electrical and thermal) was materialized in Simcenter Amesim which is a system simulation

platform widely used by aeronautics and space industries. For the gas turbine modelling a newly developed library of components, available in Simcenter Amesim, which is dedicated to the modelling and simulation of gas turbine engines (aero, industrial and marine) is used herein. The hybrid electric configuration is modelled by combining the gas turbine model with components of the electrical, control and thermal Simcenter Amesim libraries, building integrated systems capable to perform simulations both for steady state and dynamic analysis.

## 2. GAS TURBINE LIBRARY

The Gas Turbine library is consisting of relevant components such as compressor, turbine, combustor, ducts etc. The modular nature of a gas turbine engine makes the identification of components and connections a straight forward procedure. In addition to the usual components, volume components can be used for taking into account the volume dynamics effect on engine transient operation and variable orifices to simulate bleed off valves (BOV). Components from other libraries such as shafts for accounting for shaft dynamics, propellers, gearboxes, generators, heat exchangers, pumps can be combined with the gas turbine library components to allow the modelling of any gas turbine configuration and of integrated systems.

### 2.1. Components

The compressor and turbine modelling is based on the well established rigorous entropy calculations described by Walsh and Fletcher<sup>[13]</sup> and Kurzke<sup>[14]</sup>. The variable geometry effect on turbomachinery map is simulated by applying the simplified methodology described by Kurzke<sup>[14]</sup>. In this case the map parameters (mass flow (W), pressure ratio (PR) and efficiency (eff)) are corrected in accordance to eq. (1) to (3). The correction is a function of the difference of the actual variable guide vanes (VGV) position relative to the scheduled – on map- VGV position ( $\delta\text{ang}$ ) and of the relevant parameters ( $a_{VG}$ ,  $b_{VG}$ ,  $c_{VG}$ ).

$$(1) \quad \left( \frac{W\sqrt{T}}{P} \right)_{VGV} = \left( \frac{W\sqrt{T}}{P} \right)_{map} \cdot \left[ 1 + \frac{a_{VG}}{100} \delta\text{ang}(\text{deg}) \right]$$

$$(2) \quad (PR_{VGV} - 1) = (PR_{map} - 1) \cdot \left[ 1 + \frac{b_{VG}}{100} \delta\text{ang}(\text{deg}) \right]$$

$$(3) \quad \text{eff}_{VGV} = \text{eff}_{map} \cdot \left[ 1 - \frac{c_{VG}}{100} (\delta\text{ang}(\text{deg}))^2 \right]$$

Compressor and turbine maps are usually referring to a specific working medium composition (e.g. dry air). Correction terms based

on similarity can be used for accounting compositions different than the reference one. This allows assessing the effect of humidity and the effect of using different fuels. The correction terms suggested in AGARD AR-332<sup>[15]</sup> have been implemented for scaling the maps in accordance to the working medium synthesis. This feature can be activated / deactivated. For simulating turbomachinery components degradation the health indices as introduced by Stamatidis et al.<sup>[16]</sup> have been implemented. Suitable health indices can be used for simulating specific components faults<sup>[17]</sup>.

The volume dynamics and the heat transfer between the gas and the surrounding parts of the engine are represented by the chamber component with heat exchanges. The heat flow can be modelled utilizing the Amesim thermal library components and the relevant materials library. The ducts are modelled as orifices of specific flow coefficient, where the flow coefficient can be calculated via available geometrical data or imposed by the user. This approach allows for varying pressure losses throughout operation, as a function of corrected mass flow.

The combustion is modelled utilizing chemical kinetics and the relevant reaction rate coefficient<sup>[18]</sup>. Any fuel composition can be applied and the combustion products are calculated based on the stoichiometric equation. The combustion chamber components available are a primary zone component accounting for combustion and pressure drop and a secondary zone component accounting for chemical reaction and pressure drop. Both components can account for heat transfer applying thermal library components, while cooling holes can be considered too. The secondary zone can be discretized and can be used to represent the dilution zone. The fluid properties are calculated according to the NASA CEA data<sup>[19]</sup>.

The ambient air synthesis can be defined by the user in molar or mass basis. The ambient air conditions can be defined by the user or

calculated via the atmosphere component. International standard atmosphere (ISA)<sup>[20]</sup>, U.S. standard atmosphere 1976<sup>[21]</sup> and Military standard atmosphere models<sup>[22],[23]</sup> are available for selection. The ISA non-standard days are also available (hot, cold, tropical and polar) for assessing the system operation in the extremes of the design envelope.

## 2.2. Engine Model Developing

Having established a physical consistent gas turbine library any engine model can be built. The modular nature of the gas turbine engine makes this a straight forward process. In order to relate flow quantities at the inlet and outlet of individual engine components, the equations of mass and energy conservation along with species concentration conservation are employed. The equations are solved through a well established integrator switching automatically between several algorithms depending on the numerical stiffness of the system<sup>[24],[25],[26]</sup>. The gas turbine library set of components can be combined with a plethora of components of other libraries such as electrical, control and thermal, allowing the modelling of conventional and unconventional engines, the analysis of integrated systems and the application of different control strategies. A simulation environment that allows for rapid engine model implementation and evaluation can be used during the pre-design stage on an engine development programme allowing for the performance and operation assessment of new engines and configurations. A simple twin shaft engine built through drop and drag of the relevant components can be seen in Figure 1. The model control parameter is the fuel, while the power turbine rotational speed is selected to be kept constant for simulating constant rotor operation. The engine design point is defined according to Table 1.

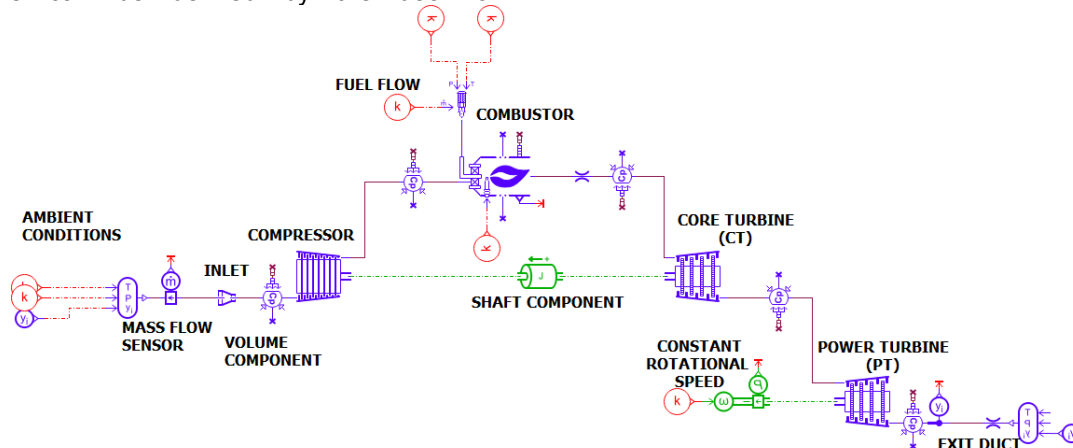


Figure 1: Twin shaft engine model

Table 1: Twin Shaft engine Design Point

Inlet duct pressure losses [%]	2.2
Compressor isentropic eff [-]	0.81
Pressure Ratio [-]	17.49
Turbine Entry Temperature [K]	1465
Combustor pressure losses [%]	6.9
Combustor efficiency [%]	98.5
Core turbine isentropic eff [-]	0.85
Power turbine isentropic eff [-]	0.85
Exit duct pressure losses [%]	9
Power [kW]	1.374

For streamlining the engine model building process a compressor and turbine map scaling tool is available. The engine design point can be derived from the open literature<sup>[27]</sup>, measurement data<sup>[28]</sup> or design calculations based on technology level<sup>[29]</sup>. The map scaling tool (Figure 2) allows for the point and click selection of the initial map design point, hence the map scaling factors<sup>[30]</sup> can be directly calculated.

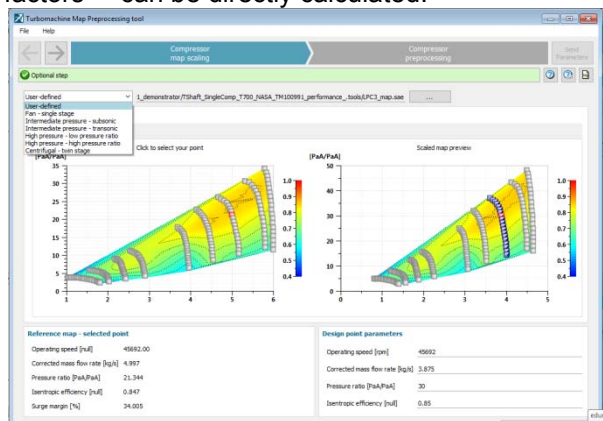


Figure 2: Compressor Map scaling tool

Having the ability to establish turbomachinery maps capable to reproduce engine operation at a specific operating range is advantageous for assessing engine performance<sup>[31]</sup> along with operability and health condition<sup>[32]</sup>. Additionally an adapted engine model can be used for assessing engine control<sup>[33],[34]</sup> and engine modifications<sup>[35]</sup>.

Indicative engine model performance data are presented in Figure 3, Figure 4 and Figure 5, along with the relevant data calculated from TURBOMATCH simulation tool. TURBOMATCH is the Cranfield University in-house 0-D performance simulation tool<sup>[36]</sup> and it has been successfully validated against experimental and simulated data<sup>[37] - [40]</sup>. The results indicate very good agreement between the two simulation tools throughout the operating range examined.

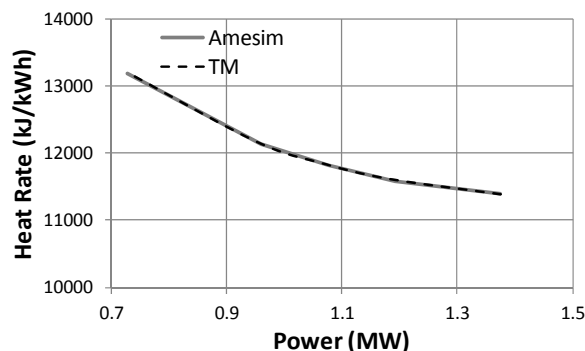


Figure 3: Heat Rate vs Power

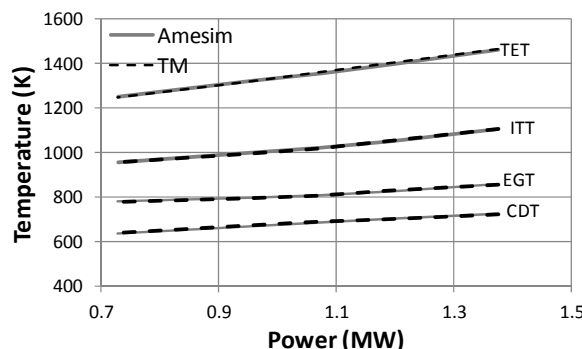


Figure 4: Engine Temperatures vs Power

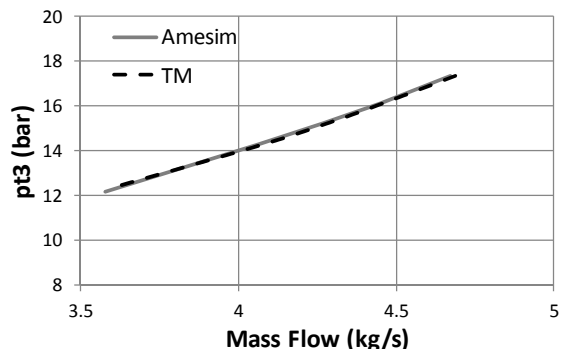


Figure 5: Compressor Operating Line

### 3. TEST CASE ENGINE

The T700-GE-700 is the first production model of the T700 family (first engine delivered in early 1978), and its civil derivatives, named as CT7<sup>[41]</sup>. It consists of a five-stage axial and a single-stage centrifugal flow compressor; a low-fuel-pressure, annular combustion chamber; a two-stage axial flow gas generator turbine; and a two-stage uncooled independent power turbine<sup>[41]</sup>. The engine model built can be seen in Figure 6, utilizing fuel flow as the setting parameter. The gas generator consists of an axial compressor (LPC) and a single centrifugal stage (HPC) driven by the core axial turbine (CT).

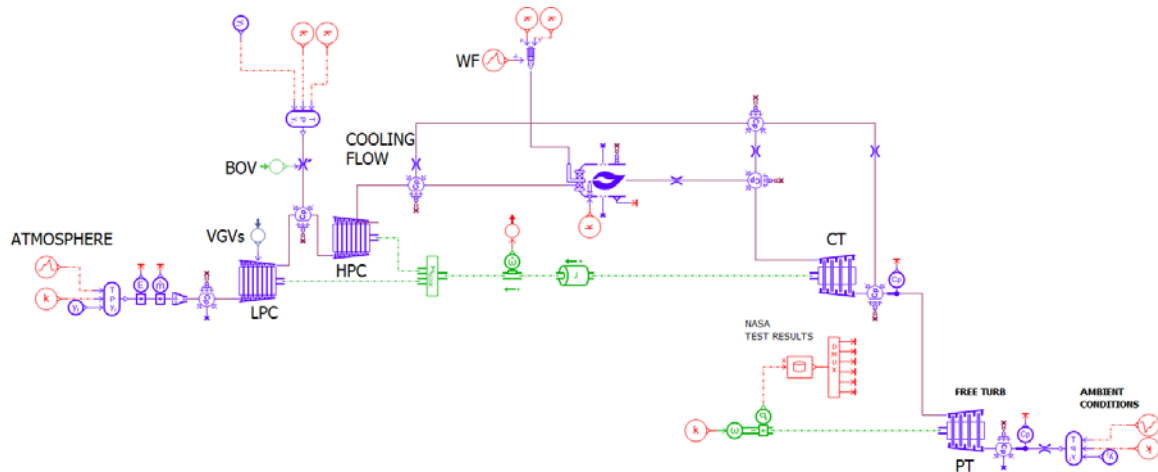


Figure 6: Amesim T700-GE-700 model configuration

The free power turbine (PT) is delivering shaft power. The model uses appropriate maps to define off-design performance for the turbomachinery components utilizing the Amesim readily available maps. The combustor pressure losses vary with the combustor inlet corrected mass flow rate. Ducts pressure losses are a function of mass flow rate. Cooling flows for the CT are extracted from the HPC exit, following the cooling flow percentage presented by Ballin<sup>[12]</sup>, while the cooling flow split is selected following the equivalent single stage cooled turbine logic<sup>[13]</sup><sup>[42]</sup> applying a work potential of the cooling flow of 0.6. The first and second stators of the T700 axial compressor are of variable geometry and the starting air is bled off from the axial compressor exit. The compressor VGV modelling is done according to eq. (1), assuming no penalty on efficiency and pressure ratio<sup>[28]</sup>. A variable BOV is also modelled applying the variable area orifice component. Both VGV and BOV position are a function of ambient temperature and rotational speed activated when the corrected gas generator speed (NG) is less than 87% of the nominal one. Kerosene (C<sub>10</sub>H<sub>20</sub>) is used as fuel in this study. The model is adapted to the experimental data presented by Ballin<sup>[12]</sup> (Table 2).

Table 2: Experimental data from NASA-Lewis experimental test engine<sup>[12]</sup>

T2 [C]	NG [%]	Np [%]	W2 [kg/s]	p3 [bar]	T3 [C]	Torque [Nm]
13.9	65.9	52.6	1.45	4.0	189.1	40.8
13.3	84.7	95.7	2.34	7.8	296.9	122.2
9.2	87.7	95.7	2.79	9.6	327.4	201.1
9.1	90.4	95.7	3.13	11.1	353.0	280.0
8.6	92.6	95.7	3.47	12.7	378.5	371.9
8.6	95.9	95.7	3.86	14.6	409.1	489.2

The adapted engine model reproduces the engine steady state experimental data with good accuracy throughout the whole operating envelope – down to 46kW, as seen in Figure 7.

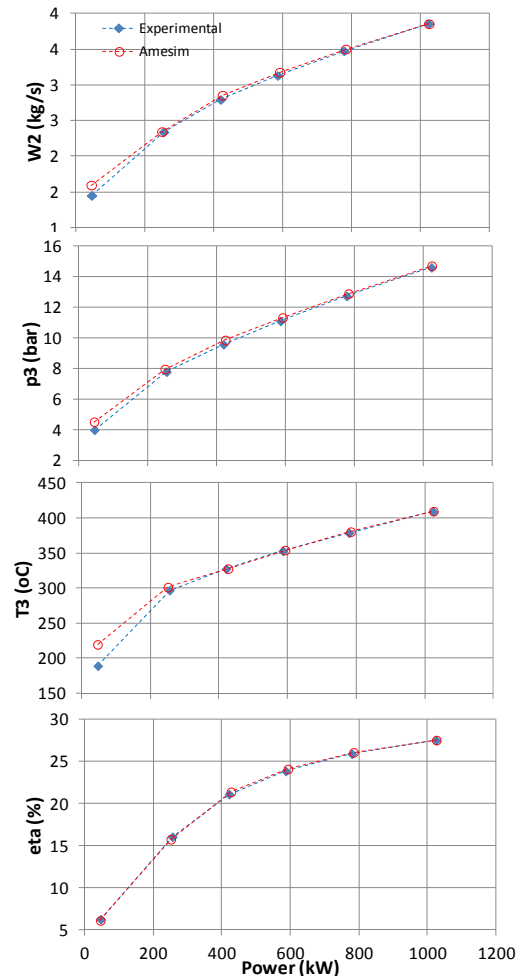


Figure 7: Measured<sup>[12]</sup> versus calculated data for steady state operation

Amesim is a dynamic simulation environment; hence the model built for steady state simulation can be directly used for transient simulation. Shaft inertia is the dominant term<sup>[43]</sup>. The gas generator and power turbine shaft moment of inertias are defined equal to 0.06033kg·m<sup>2</sup> and 0.084 kg·m<sup>2</sup> following the values recommended by Ballin<sup>[12]</sup>. The gas dynamic effects are considered utilizing the volume components. For this size of engine the gas dynamics effects are expected to be small<sup>[44]</sup>. The heat soakage effect is expected to be small<sup>[12]</sup> and it is not considered in this model. The heat soakage effect can be easily applied if relevant data is available utilizing components from the thermal and materials library.

The Amesim transient behaviour for the case of a high power manoeuvre can be seen in Figure 8 along with calculated data from the GE performance-standard status-81 simulation presented by Ballin<sup>[12]</sup>.

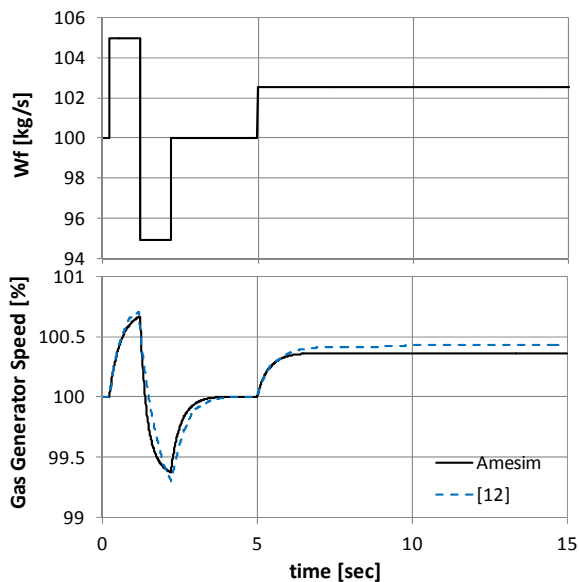


Figure 8: Simulated in<sup>[12]</sup> versus Amesim calculated data for a high power manoeuvre

The transient behaviour of the Amesim model for the case of a fuel step increase can be deduced from Figure 9. The gas generator speed, compressor discharge pressure and torque variation are presented along with calculated data from the GE performance-standard status-81 simulation presented by Ballin<sup>[12]</sup>. The power turbine speed was assumed constant in accordance with the simulation case presented by Ballin<sup>[12]</sup>.

As seen the model built in Amesim and adapted to the relevant steady state data presents the expected behaviour in terms of time constants and values for transient operation as well, thus it can be used for assessing both the steady state and transient operation of the engine.

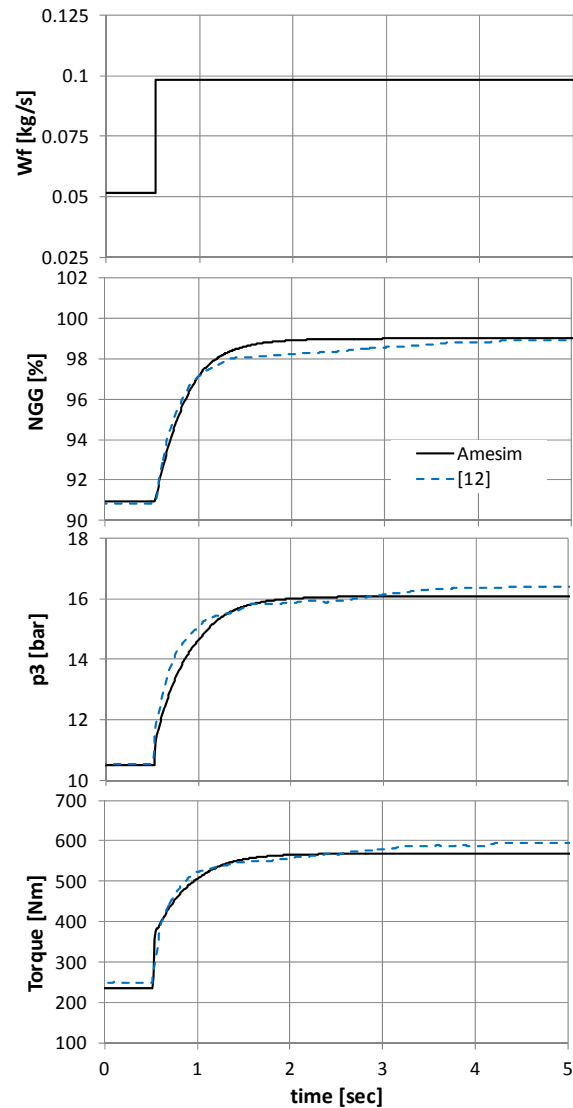


Figure 9: Simulated in<sup>[12]</sup> versus Amesim calculated data for a fuel step increase

#### 4. RECUPERATED ENGINE

Recuperated engines have been considered for rotorcraft configurations<sup>[11],[45]</sup> and assessed from a performance point of view, while the transient behaviour of the configuration has not been addressed. In this study the test case engine is acting as the baseline for the recuperated engine. The simple cycle engine model built in Amesim is easily changed to a recuperated cycle utilizing the relevant available heat exchanger components. Amesim offers several levels of modelling for the heat exchanger, depending on the available data. In this case the simplest one is selected. The heat exchanger effectiveness is assumed 70%, according to the data presented in McDonald et al.<sup>[45]</sup>. The weight and mass is calculated based on the effectiveness value applying the following

relation for the specific weight<sup>[11]</sup>:

$$(4) \quad w(\text{kg}/\text{kg}_{\text{mass flow}}) = 0.0245 \cdot [\text{eff}(\%)]^2 - 2.1985 \cdot \text{eff}(\%) + 56.64$$

The design of the heat exchanger for establishing the basic geometric information is done applying the volume calculations described by Walsh and Fletcher<sup>[13]</sup> for effectiveness of 70%. The area is calculated applying the NTU method<sup>[46]</sup>. The effectiveness is assumed to vary for off-design operation according to the following equation<sup>[13]</sup>:

$$(5) \quad \text{eff}_{\text{OD}} = 1 - \frac{W_{\text{OD}}}{W_{\text{des}}} \cdot (1 - \text{eff}_{\text{DP}})$$

The recuperated engine maximum intermittent turbine entry temperature (TET) is the one of the baseline engine. The engine intermittent shaft power is decreased by almost 19% due to the additional pressure losses imposed by the heat exchanger from 1210kW to 982kW. This decrease would be prohibitive in a typical configuration, but in the case of hybrid propulsion the additional power can be provided by the batteries. On the other hand the recuperated engine presents betterment in specific fuel consumption equal to 14% at high load operation, as can be seen in Figure 10. The fuel consumption improvement is greater when part load operation is considered. The maximum continuous rating (MCR) of the simple cycle engine is equal to 987kW<sup>[47]</sup>. For the recuperated engine the power produced for the same TET is 832kW. The recuperated engine has specific fuel consumption (sfc) of 254 g/kWh, decreased by 15.7% compared to the simple cycle engine MCR.

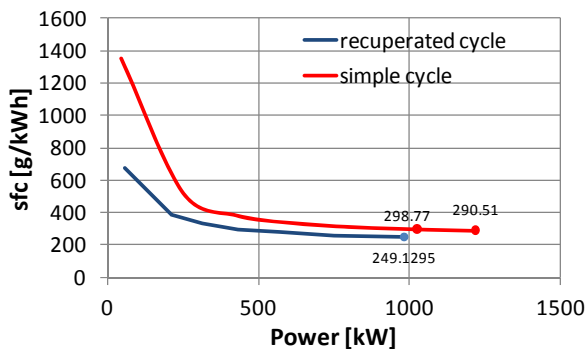


Figure 10: simple and recuperated cycle performance

The addition of the heat exchanger changes the response time of the gas turbine to external disturbances, as expected<sup>[48]</sup>, due to the recuperator volume and thermal inertia. The effect of the recuperator to the transient behaviour of the engine can be seen in Figure 11. The lag is a strong function of thermal inertia; hence more

detailed heat exchanger design is needed for fully assessing its effect on the overall engine transient operation. Nevertheless, it is apparent that the recuperated model captures the physics and general trends can be derived.

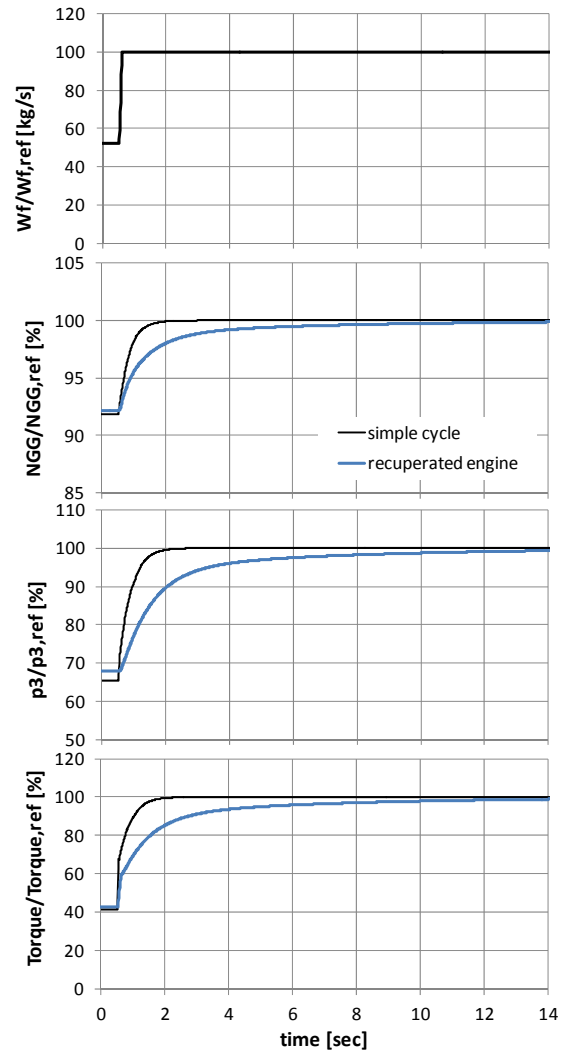


Figure 11: simple cycle and recuperated engine response to a fuel step increase

Recuperation increases the pressure ratio of the engine for a specific operating point due to the increased pressure losses; hence it is expected to negatively affect the compressors surge margin. Thermal inertia is also expected to negatively affect surge margin during transient operation. For quantifying these effects on surge margin, an acceleration – deceleration manoeuvre is simulated (Figure 12). As seen in Figure 13 and Figure 14 the surge margin of the recuperated engine reduces significant compared to the simple cycle. As expected the time lag due to the recuperator thermal inertia is significantly more profound than the effect of shaft inertia. This behaviour highlights the importance of examining the engine operability along with the performance

when new configurations or modifications are assessed.

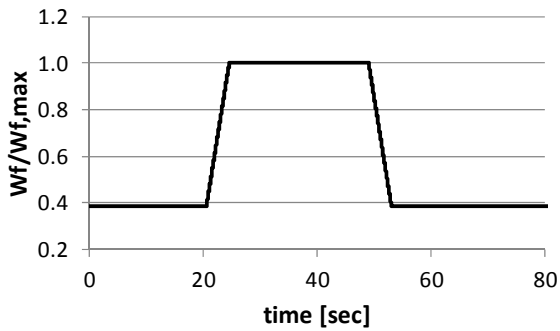


Figure 12: fuel step increase relative to maximum

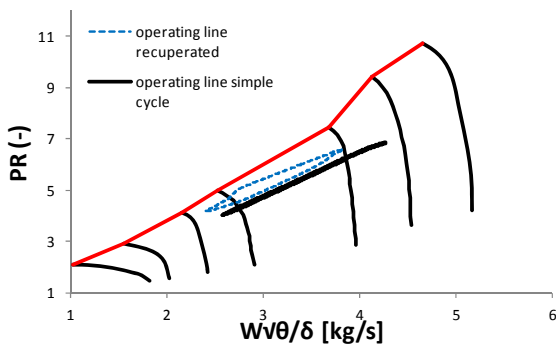


Figure 13: simple cycle and recuperated engine response to a fuel step increase – axial compressor

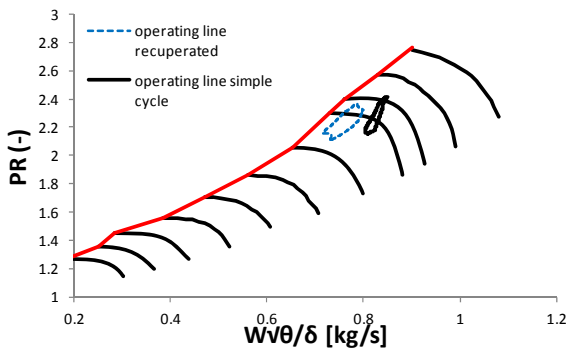


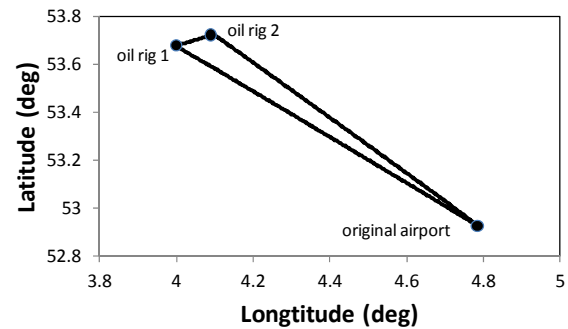
Figure 14: simple cycle and recuperated engine response to a fuel step increase – centrifugal compressor

## 5. THERMO-ELECTRIC POWERPLANT ASSESSMENT

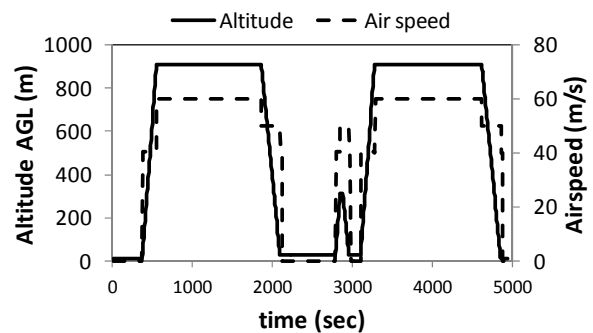
### 5.1. Helicopter mission definition

For performing the preliminary assessment of the recuperated engine a typical TEM helicopter is used as a test case. HECTOR has been used for deriving the power demand for a specified mission. HECTOR is an in-house rotorcraft comprehensive code<sup>[49]</sup> that has been used to

reproduce with good accuracy power requirements for TEM helicopters<sup>[50],[51]</sup>. An Oil and Gas (OAG) mission representative of modern TEM helicopter operation has been defined. The schedule assumes that the helicopter takes off from De Kooy Airfield in Den Helder, the Netherlands while carrying a specified payload. The helicopter subsequently travels towards a designated offshore oil/gas platform (oil rig 1) located in the North Sea, where it lands and drops off the on-board payload. The helicopter then travels towards a second offshore oil/gas platform (oil rig 2) where it picks up another useful payload and subsequently returns to the original De Kooy Airfield in Den Helder. Climb and descent rates are held fixed at 5 m/s and 3.5 m/s, respectively. A time step  $Dt$  of 5 s is used for each individual mission segment. All coordinated turns are executed with a turn rate of 5 deg/s, with the exception of fine tuning of the helicopter's orientation, where the turn rate is defined based on the orientation error and the mission time step  $Dt$ . The mission range is 206.8km and the time is 4935sec, the on-board payload is assumed equal to 616kg and the initial Take Off Weight (TOW) is equal to 5000kg.



(a)



(b)

Figure 15: OAG mission: (a) geographical definition; (b) time variations of deployed operational airspeed and height above ground level altitude

The power demand for the mission, for TOW of 5000kg is depicted in Figure 16.

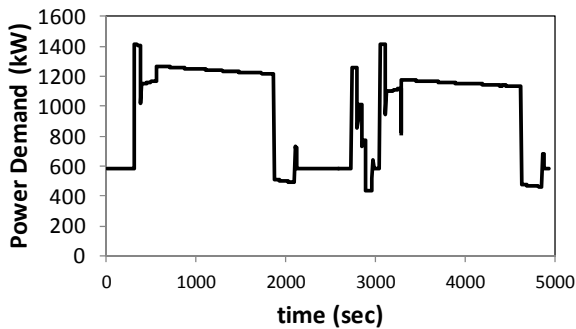


Figure 16: OAG mission total power demand

## 5.2. Propulsion system

A series hybrid configuration is modelled in Amesim utilizing components from the electric motor library. The recuperated gas turbine is connected to a generator providing power to the motor and charging the batteries. The batteries also provide energy to the motor during one or more phases, supplementing the engines available power. The motor is connected to the helicopter rotor. The battery considered has a nominal capacity of 75Ah and a nominal voltage of 270V<sup>[52]</sup>. The Amesim available battery sizing tool<sup>[53],[54]</sup> has been used, while the option to import data from datasheets is available. For this preliminary study the simplest Amesim generator component is used. It is sized based on the maximum torque and rotational speed. Efficiency is assumed constant throughout operation and equal to 0.98<sup>[55]</sup>. The quasi static model of Permanent Magnet Synchronous Machine (PMSM) has been used for the motor along with the relevant controller, selecting varying winding losses. The controller efficiency is assumed constant and equal to 0.97<sup>[55]</sup>. The integrated

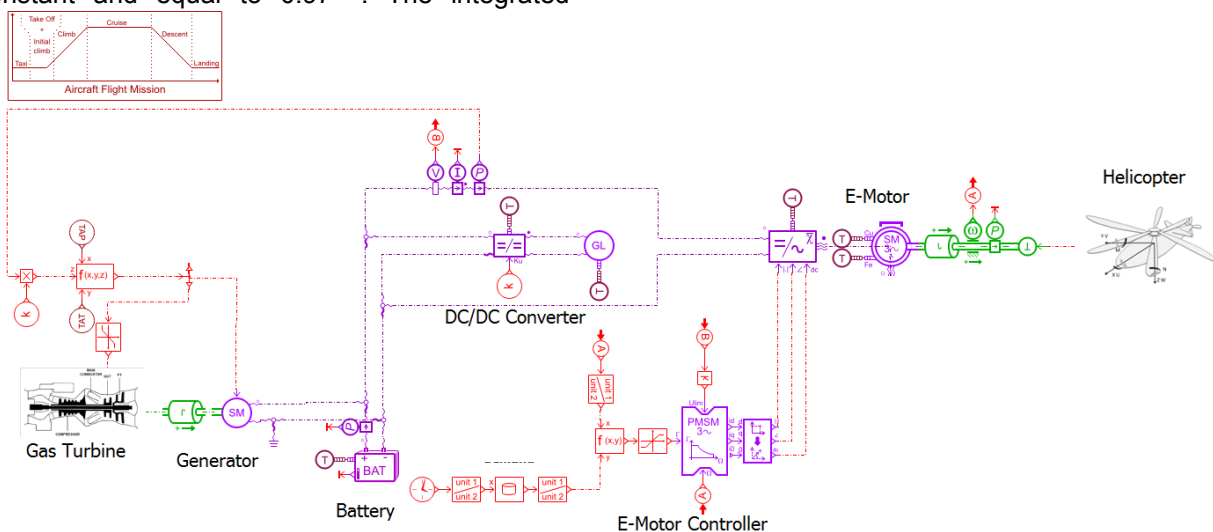


Figure 17: Amesim Series hybrid configuration

series hybrid configuration built can be seen in Figure 17. The electric power system is connected to the helicopter component which provides the torque demand of the helicopter as calculated by HECTOR. The power source is the gas turbine, as seen in Figure 17. The gas turbine and the helicopter torque request are depicted as supercomponents for Figure clarity. The relevant models are accessible in the hybrid configuration by just opening the relevant supercomponent. The simple cycle engine is directly connected to the helicopter component, thus only the gearbox losses are applied. A simplistic engine control scheme has been developed in order to: a) provide the fuel flow needed for the specified power and b) keep the TET lower than a specified value. The true airspeed and altitude are mission inputs in the relevant component. The mission component calculates the atmosphere conditions (total and static) that are used as input to the engine model.

## 5.3. Performance and Operability analysis

The OAG mission has been simulated in Amesim both for the conventional configuration: simple cycle with gearbox and for the hybrid configuration: recuperated cycle with series hybrid propulsion system. For the series hybrid case the engine is charging the batteries if the state of charge (SOC) of the batteries is less than 100% and the engine has power surplus. For the mission the engines are bounded by the corresponding MCR.

In case of the hybrid configuration, when the actual TET becomes greater than the MCR TET, the fuel is stabilized and the battery is supporting the engine, providing the additional power.

The OAG mission is simulated for different TOW ranging from 5000kg to 6260kg to quantify the effect of the helicopter weight on the fuel consumption and system operation. The results are presented in Table 3. Along with the mission fuel (block fuel) the overall energy ratio defined as the ratio between the electrical energy used for propulsion to the overall propulsion energy is calculated.

$$(6) \quad E_{ov}(\%) = \frac{\int_{t=0}^t P_{el} \cdot dt}{\int_{t=0}^t P_{prop} \cdot dt} \cdot 100$$

Additionally the maximum ratio of electrical power to propulsion power calculated during the mission is calculated.

$$(7) \quad PR_{el}(\%) = \left( \frac{P_{el}}{P_{prop}} \cdot 100 \right)_{\max} \Big|_{t=0}^t$$

As seen in Table 3 the addition of the recuperator gives a significant block fuel benefit. This benefit originates from the positive thermodynamic effect of recuperation and from the fact that the recuperated engine operates more time to higher power setting, hence to regions of better efficiency. This explains why the benefit of the recuperation on the fuel burn decreases slightly as the TOW increases (from 17.5% to 16%) since the simple cycle engine operates at higher power settings and hence at lower sfc as the TOW increases. In any case the benefit on block fuel is greater than the improvement on MCR sfc, since the operating point benefit is added to the thermodynamic benefit.

For TOW less than 5500kg the battery is not used. As the TOW increases, the recuperated engines are unable to produce the propulsion power needed throughout the mission without increasing the TET. Since a maximum value of TET is imposed the utilization of the battery increases. For TOW of 6260kg almost 9% of the

total propulsion energy comes from the battery. For this case the maximum battery produced propulsion power at a specific operating point during the mission is 18% of the total propulsion power.

For further assessing the series hybrid configuration performance the propulsion system weight should be considered as a parameter. As discussed in several publications<sup>[52] [55] [56] [57]</sup> there is much uncertainty in the specific power of the future generators/motors and batteries, hence herein three cases will be examined. The battery energy density is assumed 250 Wh/kg [56], resulting to a weight of 81kg. The envisioned generators/motors energy density varies from 5kW/kg to 30kW/kg<sup>[56] [57] [58]</sup>, thus a pessimistic approach may be 5kW/kg and an optimistic approach 30kW/kg. Assuming a 5kW/kg power density the electric system weight, based on maximum total power setting of 2500kW is estimated 1081kg and the recuperated propulsion system total weight is estimated equal to 1241kg (Case A). If an in-between value of 10kW/kg is used then the total recuperated propulsion system total weight is estimated equal to 741kg (Case B) and if an optimistic power density of 30kW/kg is applied then the total weight is estimated equal to 408kg (Case C). The block fuel change relative to the simple cycle configuration in relation to the added weight for the OAG mission is presented in Figure 18. Case A has a detrimental effect on fuel consumption, since the added weight overcomes the benefits of recuperation and high power setting operating point. Case B, gives a benefit of 5.2% for the whole mission, indicating that a series hybrid recuperated configuration may have a positive effect on mission fuel consumption in the near future. Case C gives a benefit of more than 10% with respect to block fuel, since it is the most optimistic case. The added weight for which the fuel benefit for the specific mission is zeroed is 1085kg.

Table 3: Overall mission results for different TOW

	TOW [kg]	5000	5160	5360	5560	5760	5960	6260
<b>simple cycle</b>	<b>Block Fuel [kg]</b>	488.2	498.6	516.5	536.0	555.4	567.8	598.6
	<b>Block Fuel [kg]</b>	402.7	412.2	428.5	446.5	464.2	475.5	503.2
<b>recuperated cycle</b>	<b>PR<sub>el</sub> [%]</b>	0	0	0	2.18	7.63	9.91	18.03
	<b>E<sub>ov</sub> [%]</b>	0	0	0	0.74	2.53	4.40	8.91

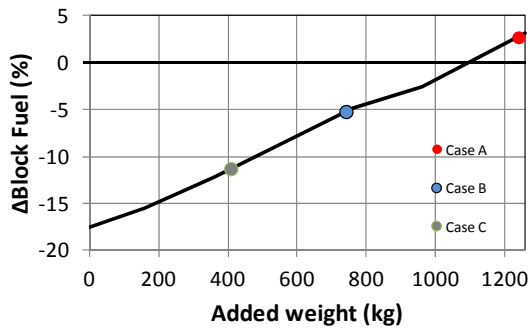


Figure 18: OAG Mission fuel versus added weight

Concerning the engine operability, the engine operating points throughout the mission are depicted in Figure 19 and Figure 20 for the case of TOW 5960kg. It is apparent that the recuperated engine lag is greater than that of the simple cycle engine, while the engine pressure increased pressure drop moves the operating line towards the surge line. Specifically the surge margin is reduced by approximately 30% for the axial compressor and by 50% for the centrifugal compressor, mostly due to the engine transient operation. This behaviour indicates that the response of the recuperated engine on fast transient should be further examined for further assessing the viability of the configuration. Nevertheless for the mission examined the recuperated engine operates in the stable region.

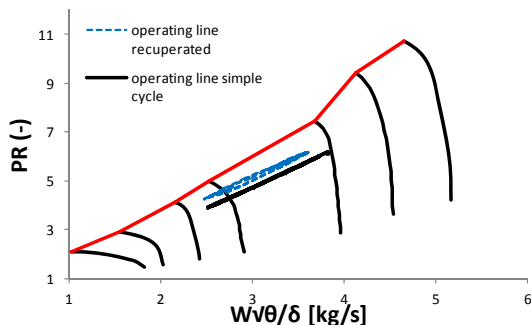


Figure 19: operating points throughout the OAG mission – axial compressor

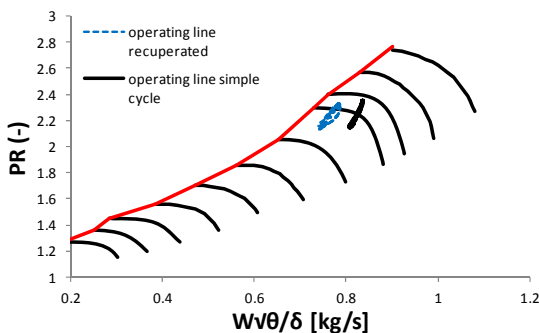


Figure 20: operating points throughout the OAG mission – centrifugal compressor

## 6. CONCLUSIONS

A series hybrid propulsion system utilizing a recuperated gas turbine configuration is assessed. Firstly a fully adapted engine model capable to reproduce an engine steady state and transient operation is built and used as a baseline for the recuperated engine. The results indicate that the model built in Amesim and adapted to the relevant steady state data presents the expected behaviour in terms of time constants and values for transient operation as well, thus it can be used for assessing both the steady state and transient operation of the engine. Following a recuperated version of the simple cycle engine is built and simulated. The expected behaviour is observed. The recuperated engine offers approximately 16% better sfc at the expense of available power. During transient manoeuvres the recuperated engine is lagging compared to the simple cycle due to the recuperator thermal inertia. The time for achieving steady state increases for a specific manoeuvre from less than 2 s for the simple cycle to almost 12 s for the recuperated one, for the heat exchanger mass calculated through the preliminary weight evaluation. Additionally the recuperated engine operates to significant lower surge margin compared to the simple cycle. Having established a recuperated version of the engine a series hybrid configuration utilizing the recuperated engine is built in Amesim and assessed in terms of performance and engine operability. An OAG mission is used for comparing the simple gas turbine cycle and the hybrid configuration. The hybrid recuperated configuration offers a fuel economy in the range of 17% if the weight penalty is neglected. As the TOW increases the electric propulsion energy increases. For the case of TOW 6260kg, almost 9% of the propulsive energy comes from the battery, with a maximum instant power contribution of 18%. These results indicate that the hybrid propulsion may be an enabling technology for making recuperated configurations appealing. For assessing the hybrid configuration the weight penalty imposed by the electric power system and the heat exchanger weight is addressed. Three cases, relative to the electric components power density are defined: one pessimistic, one plausible and one optimistic. The plausible one refers to envisioned 2025 technology. The configuration assessed indicates that the block-fuel benefit of the series hybrid configuration for the 2025 case is expected to be around 5%. This value indicates that hybridization may support the introduction of recuperated engines in rotorcraft propulsion utilizing existing engine designs reducing the development time and cost.

## 7. REFERENCES

- [1] Airbus, 2016, "Global Market Forecast, Mapping Demand 2016/2035," Technical report
- [2] D'Ippolito, R., Stevens, J., Pachidis, V., Berta, A., Goulos, I., and Rizzi, C., 2009, "A Multidisciplinary Simulation Framework for Optimization of Rotorcraft Operations and Environmental Impact," 2nd International Conference on Engineering Optimization (EngOpt 2010), Lisbon, Portugal, September, 2010, pp. 6-9.
- [3] Green Rotorcraft, Clean Sky, accessed on 05/08/2018: <http://www.cleansky.eu/green-rotorcraft-grc>
- [4] Clarke, J.-P., "The role of advanced air traffic management in reducing the impact of aircraft noise and enabling aviation growth", Journal of Air Transport Management, Vol. 9, No. 3, may 2003, pp. 161-165.
- [5] Kirner R., Raffaelli L., Rolt A., Laskaridis P., Douleris G. & Singh R. (2015) An assessment of distributed propulsion: Advanced propulsion system architectures for conventional aircraft configurations, Aerospace Science and Technology, 46 42-50.
- [6] Voskuijl, M., van Bogaert, J. and Rao, A. G. (2017) 'Analysis and Design of Hybrid Electric Regional Turboprop Aircraft', CEAS Aeronautical Journal. Springer Vienna, 9(1), pp. 15–25. doi: 10.1007/s13272-017-0272-1.
- [7] Bradley M, Droney C, Paisley D, Roth B, Gowda S, Kirby M. "NASA N+3 Subsonic Ultra Green Aircraft Research SUGAR Final Review", Boeing Research and Technology, 2010
- [8] Vratny C. P., Forsbach F., Seitz A., Hornung M., 2014, "Investigation of Universally Electric Propulsion Systems for Transport Aircraft", 29th Congress of the International Council of the Aeronautical Sciences at: St. Petersburg, Russia
- [9] Kailos N. C., "Increased helicopter capability through advanced power plant technology", Journal of the American Helicopter Society, Volume 12, Number 3, 1 July, pp. 1-15(15).
- [10] Privoznik, E. J., 1968, "Allison T63 Regenerative Engine Program", Journal of the American Helicopter Society, Volume 13, Number 4, 1 October 1968, pp. 56-63(8)
- [11] Fakhre A., Goulos I & Pachidis V (2015) An integrated methodology to assess the operational and environmental performance of a conceptual regenerative helicopter, Aeronautical Journal - New Series-, 119 (1211) 1-24.
- [12] Ballin M. G. A High Fidelity Real-Time Simulation of a Small Turboshaft Engine. Technical report, NASA Ames Research Center, 1988.
- [13] Walsh, P.P. and Fletcher, P., 2004, Gas Turbine Performance, 2nd Edition, Blackwell Science, Oxford.
- [14] Kurzke J., 2007, "About Simplifications in Gas Turbine Performance Calculations", ASME paper No. GT2007-27620, Proceedings of GT2007, ASME Turbo Expo 2007: Power for Land, Sea and Air, May 14-17, 2007, Montreal, Canada
- [15] AGARD-AR-332, 1995, "Recommended Practices for the Assessment of the Effects of Atmospheric Water Ingestion on the Performance and Operability of Gas Turbine Engines", North Atlantic Treaty Organization.
- [16] Stamatis, A., Mathioudakis, K., Smith, M., Papailiou, K.D., "Gas Turbine Component Fault Identification by Means of Adaptive Performance Modelling". ASME Paper 90-GT-376, 1990
- [17] Basendwah A. A., Pilidis P., Li Y. G., "Turbine Off- Line Water Wash Optimization Approach for Power Generation", ASME paper No. GT2006-90244
- [18] A.H. Lefebvre and D.R. Ballal, Gas Turbine Combustion, Alternative fuels and emissions, 3rd ed., Taylor and Francis Group, LLC, 2010
- [19] Bonnie J. McBride, Michael J. Zehe and Sanford Gordon, "NASA Glenn Coefficients for Calculating Thermodynamic Properties of Individual Species". NASA/TP-2002-211556, 2002
- [20] International Organization for Standardization, Standard Atmosphere, ISO 2533:1975, 1975.
- [21] U.S. Standard Atmosphere 1976 (NASA-TM-X-74335)
- [22] MIL-STD-3013, Glossary of definitions, ground rules, and mission profiles to define air vehicle performance capability (14 Feb 2013).
- [23] MIL-HDBK-310, Military Handbook: Global climatic data for developing military products (23 Jun 1997).
- [24] Brenan KE, SL Campbell & LR Petzold, Numerical Solution of Initial-Value problems in Differential-Algebraic Equations, North-Holland, 1989.
- [25] Lapidus L & J Seinfeld, Numerical Solution of Ordinary Differential Equations, Academic Press, 1971.
- [26] Petzold LR, Automatic Selection of Methods for Solving Stiff and Nonstiff Systems of Ordinary

- Differential Equations, SIAM J. Sci. Comput., 4, 1983.
- [27] Roumeliotis I.; Aretakis N.; Mathioudakis K., 2003, "Performance Analysis of Twin-Spool Water Injected Gas Turbines Using Adaptive Modelling", Proc. ASME. 36843; Volume 1: Turbo Expo 2003:861-870. January 01, 2003, GT2003-38516
- [28] Roumeliotis I., Aretakis N., Alexiou A., 2017, "Industrial Gas Turbine Health and Performance Assessment With Field Data", ASME J. Eng. Gas Turbines Power 139(5)
- [29] Nkoi B., Pilidis P., Nikolaidis T., "Performance assessment of simple and modified cycle turboshaft gas turbines", Propulsion and Power Research, Volume 2, Issue 2, June 2013, Pages 96-106
- [30] Pachidis, V., The Turbomatch scheme; for aero/industrial gas turbine engine design point/off design performance calculation, Manual, Cranfield University, UK, October 1999.
- [31] Xu L., Kyprianidis G. K., Grönstedt U. J. T. "Optimization Study of an Intercooled Recuperated Aero-Engine", Journal of Propulsion and Power, Vol. 29, No. 2 (2013), pp. 424-432.
- [32] Aretakis N., Roumeliotis I., Alexiou A., Romesis C., Mathioudakis K., 2014, "Turbofan Engine Health Assessment From Flight Data", ASME J. Eng. Gas Turbines Power 137(4)
- [33] Perez-Blanco H., Henricks B. T., 1998, "A Gas Turbine Dynamic Model for Simulation and Control" Paper No. 98-GT-078, ASME 1998 International Gas Turbine and Aeroengine Congress and Exhibition, Stockholm, Sweden, June 2-5, 1998
- [34] Kim, J. H., Song, T. W., Kim, T.S. and Ro, S.T., 2001, Model Development and Simulation of Transient Behaviour of Heavy Duty Gas Turbines, ASME Journal of Engineering for Gas Turbines and Power, 123, pp. 589-594
- [35] Tsiokas S., Roumeliotis I., Aretakis N., Alexiou A., 2014, "Assessment of the Conversion of a Helicopter Engine for Electrical Power Production", Nausivios Chora, Ed. 2014, 15 pages
- [36] Macmillan W. L., Development of a Modular Type Computer Program for the Calculation of Gas Turbine Off-Design Performance, PhD Thesis, Cranfield Inst. of Technology, 1974.
- [37] P. Giannakakis, P. Laskaridis, T. Nikolaidis and A. Kalfas, "Toward a Scalable Propeller Performance Map," AIAA / Journal of Propulsion and Power, vol. 31, no. 4, pp. 1073-1082, 2015.
- [38] V. Pachidis, P. Pilidis, L. Marinai and I. Templalexis, "Towards a full two dimensional gas turbine performance simulator," Aeronautical Journal, vol. 111, no. 1121, pp. 433-442, 2007.
- [39] Y. G. Li, L. Marinai, E. L. Gatto, V. Pachidis and P. Pilidis, "Multiple-Point Adaptive Performance Simulation Tuned to Aeroengine Test-Bed Data," Journal of Propulsion and Power, vol. 25, no. 3, pp. 635-641, 2009.
- [40] Pellegrini A., Nikolaidis T., Pachidis V., Köhler S., "On The Performance Simulation Of Inter-Stage Turbine Reheat", Applied Thermal Engineering Volume 113, 25 February 2017, Pages 544-553
- [41] Gunston B. Jane's Aero-Engines. 1996. General Electric Aircraft Engine Business Group. Model Specification for T700-GE-700 Turboshaft Engine, Part I. Technical report, 1983.
- [42] Kurzke, J., 2002, 'Performance Modelling Methodology: Efficiency Definitions for Cooled Single and Multistage Turbines', GT-2002-30497
- [43] Horobin, M. S., 1999, Cycle-match engine models used in functional engine design – an overview, RTO Meeting Proceedings: MP-8 Design Principles and Methods for Aircraft Gas Turbine Engines, pp. 44.1-44.22
- [44] Maria V. C., Garcia Rosa, N. , Carbonneau X., (2016), "Sensitivity Analysis and Experimental Validation of Transient Performance Predictions for a Short-Range Turbopan", ASME paper No. GT2016-57257 In: ASME Turbo Expo, 13 June 2016 - 17 June 2016
- [45] Colin F. McDonald, Aristide F. Massardo, Colin Rodgers, Aubrey Stone, (2008) "Recuperated gas turbine aeroengines, part II: engine design studies following early development testing", Aircraft Engineering and Aerospace Technology, Vol. 80 Issue: 3, pp.280-294
- [46] Incropera P. F., DeWitt P. D., Bergman L. T., Lavine S. A., 2006, "Fundamentals of Heat and Mass Transfer"
- [47] Gunston B. Jane's Aero-Engines. 1996.
- [48] Kim, J. H., Kim, T. S. and Ro, S.T., 2001, Analysis of the dynamic behaviour of regenerative gas turbines, Proc Instn Mech Engrs, 215 A, J. Power and Energy, pp. 339-346.
- [49] Goulos I., 2012, "Simulation Framework Development for the Multidisciplinary Optimization of Rotorcraft", Ph.D. Thesis, Cranfield University, Cranfield
- [50] Carretero J. O., Pardo C. A., Goulos I., Pachidis V., 2018, "Impact of Adverse Environmental Conditions on Rotorcraft Operational Performance and Pollutant

Emissions”, ASME Journal of Engineering for Gas Turbines and Power, 140 (13 pages)

[51] Goulos I., Giannakakis P., Pachidis V., Pilidis P., 2013, “Mission Performance Simulation of Integrated Helicopter–Engine Systems Using an Aeroelastic Rotor Model”, J. Eng. Gas Turbines Power 135(9), 091201 (Jul 31, 2013)

[52] Donateo T., Ficarella A., Spedicato L., 2018, “Applying Dynamic Programming Algorithms to the Energy management of Hybrid Electric Aircraft”, ASME paper No. GT2018-76500

[53] Marc N. 2013, “Méthodologie de dimensionnement d'un véhicule hybride électrique sous contrainte de minimisation des émissions de CO<sub>2</sub>”, Université d'Orléans,

[54] Petit M., Marc N., Badin F., Mingant R., Sauvant-Moynot V., “A Tool for Vehicle Electrical Storage System Sizing and Modelling for System Simulation”, 2014 IEEE Vehicle Power and Propulsion Conference (VPPC), Coimbra, p. 91-96.

[55] Enconniere J., 2017, “Performance Analysis Of An Integrated Thermo-Electric Powerplant For Rotorcraft Operations”, PhD Thesis, Cranfield University, School of Aerospace, Transport and Manufacturing, Centre for Propulsion

[56] Hepperle, M., “Electric Flight - Potential and Limitations,” NATO, No. STO-MP-AVT-209, 2012

[57] Brown, G. V., “Weights and efficiencies of electric components of a turboelectric aircraft propulsion system” 49th AIAA Aerospace Sciences Meeting. Orlando, 2011.

[58] Gibson, A., Hall, D., Waters, M., Masson, P., Schiltgen, B., Foster, T., and Keith, J., “The Potential and Challenge of TurboElectric Propulsion for Subsonic Transport Aircraft” 48th AIAA Aerospace Sciences Meeting Including the New Horizons Forum and Aerospace Exposition, American Institute of Aeronautics and Astronautics, Reston, Virginia, jan 2010.